



## Effects of short-term variability of meteorological variables on soil temperature in permafrost regions

Christian Beer<sup>1,2</sup>, Philipp Porada<sup>1,2</sup>, Altug Ekici<sup>1,3</sup>, and Matthias Brakebusch<sup>1,2</sup>

<sup>1</sup>Department of Environmental Science and Analytical Chemistry (ACES), Stockholm University, 10691 Stockholm, Sweden

<sup>2</sup>Bolin Centre for Climate Research, Stockholm University, 10691 Stockholm, Sweden

<sup>3</sup>Uni Research Climate, Bjerknes Centre for Climate Research, Bergen, Norway

*Correspondence to:* Christian Beer ([christian.beer@aces.su.se](mailto:christian.beer@aces.su.se))

**Abstract.** Effects of the short-term temporal variability of meteorological variables on soil temperature in northern high latitude regions have been investigated. For this, a process-oriented land surface model has been driven using an artificially manipulated climate dataset. Climate variability mainly impacts snow depth, and the thermal diffusivity of lichens and bryophytes. This latter effect is of opposite direction in summer and winter in most regions. These impacts of climate variability on insulating surface layers together substantially alter the heat exchange between atmosphere and soil. As a result, soil temperature is 0.1 to 0.8 °C higher when climate variability is reduced. Earth system models project warming of the Arctic region but also increasing variability of meteorological variables and more often extreme meteorological events. Therefore, our results show that projected future increases in permafrost temperature and active-layer thickness in response to climate change will be lower i) when taking into account future changes in short-term variability of meteorological variables, and ii) when representing dynamic snow and lichen and bryophyte functions in land surface models.

### 1 Introduction

Soil temperature is an important physical variable of a terrestrial ecosystem since it controls many functions of microbes and plants. In permafrost regions, soil temperature also defines the biologically active part of the soil that is thawing in summer (active layer). Therefore, impacts of future warming on soil temperature have been investigated in numerous experimental and modelling studies during the past decades. Large-scale soil temperature is mainly determined by vertical heat conduction. Therefore, soil temperature usually follows an annual sinusoidal cycle of air temperature with



a damped oscillation (Campbell and Norman, 1998). That is why the projected large increase in air temperature in the Arctic region over the next 100 years (Ciais et al., 2013) is raising large concerns about the response of soil temperature and hence permafrost thawing in the Arctic. Indeed, measurements during the last decades already show an increasing permafrost temperature (Romanovsky et al., 2010) and active-layer thickness (Callaghan et al., 2010) in response to global warming. Also, first modelling results confirm such simple response of increasing future soil temperature and active-layer thickness (Schaefer et al., 2011; Koven et al., 2011; Lawrence et al., 2012; Peng et al., 2016). As a result of increasing soil temperature and active-layer thickness, heterotrophic respiration is suggested to increase because of the temperature-response of biochemical functions (Arrhenius, 1889; van't Hoff, 1896; Lloyd and Taylor, 1994) and the additional availability of decomposable substrate (Schaphoff et al., 2013; Koven et al., 2015) potentially leading to a positive climate-carbon cycle feedback (Zimov et al., 2006; Beer, 2008; Heimann and Reichstein, 2008).

Meteorological variables, such as air temperature and precipitation will not only change gradually into the future but also their short-term variability and frequency of extreme events is projected to change (Easterling et al., 2000; Rahmstorf and Coumou, 2011; Seneviratne et al., 2012). For instance, for northern high-latitude regions, climate models project an increase of the annual maximum of the daily maximum temperature by 4 °C by 2100 (Seneviratne et al., 2012) while annual maximal daily precipitation is projected to increase by 20% in these areas by 2100. At the same time, many ecosystem functions respond non-linearly to environmental factors, cf. for instance the temperature-dependence of biochemical functions (Arrhenius, 1889). Therefore, effects of the short-term (daily to weekly) variability of meteorological variables on the long-term (decadal) mean ecosystem functions can enhance or dampen the effect of a general gradual warming (Reichstein et al., 2013; Schwalm et al., 2017). That is why there is a strong need to understand such effects of climate variability on ecosystem states and functions in addition to gradual changes in order to reliably project future ecosystem state dynamics and climate. In this context, effects of climate variability on soil temperature in northern high latitude environments have not been studied so far: In addition to a gradual warming of Arctic air and soil temperature, what are the specific effects of changing short-term variability of meteorological variables on the long-term mean annual or seasonal soil temperature? Will a short-term variability change have the capability to enhance or dampen the anticipated soil warming?

Due to the well-known dampening effects of snow, near-surface vegetation, and the organic layer (Yershov, 1998, pages 361-369) (Goodrich, 1982; Zhang, 2005; Wang et al., 2016; Jafarov and Schaefer, 2016), one would expect no to little additional effects of changing air temperature fluctuations on soil temperature, in particular not on subsoil and permafrost temperature. However, air temperature variability will have an impact on snow height indirectly through snow density (Abels, 1892) and also directly when temperature is periodically rising above the melting point. In addition, the dependence of soil and near-surface vegetation conductivity on water and ice content (Camp-



bell and Norman, 1998) complicates the picture because water and ice contents themselves are also temperature-dependent. Snow manipulation experiments have proven the large *spatial* heterogeneity  
60 of soil temperature in cold regions due to snow height heterogeneity (Wipf and Rixen, 2010). The temporal variability of insulating layers and their properties should be of similar importance for soil temperature.

At high latitudes, near-surface vegetation consists to a large part of lichens and bryophytes, which often form a continuous layer on the ground. Lichens are symbiotic organisms consisting of a fungus  
65 and at least one green alga or cyanobacterium, while bryophytes are non-vascular plants which have no specialised tissue such as roots or stems. Both groups cannot actively control their water uptake and loss, but they tolerate drying and are able to reactivate their metabolism on rewetting. Typical species of upland regions at high latitudes are feather mosses such as *Hylocomium splendens* and *Pleurozium schreberi* or the lichen *Cladonia stellaris*. This near-surface vegetation is growing on  
70 top of any organic horizon and hence important for heat fluxes between land and atmosphere. In particular also for this layer, thermal and hydrological properties depend highly on water and ice content. Hence, lichens and bryophytes dynamically influence the vertical heat conduction (Porada et al., 2016a).

This study investigates the effects of *temporal* variability of meteorological variables on snow and  
75 lichen/bryophyte insulating properties and hence soil temperature in permafrost regions. For this, a recently advanced land surface model (LSM) has been used that also represents permafrost-specific processes, and in particular a dynamic snow representation and a dynamic near-surface vegetation model (Porada et al., 2016a). While the model has been evaluated against several types of observations in other studies (Ekici et al., 2014, 2015; Porada et al., 2016a; Chadburn et al., 2017), here  
80 mean annual ground temperature (MAGT) is evaluated again against different observations or other modelling studies. Then, the model is run with two distinct climate forcing datasets, one control dataset and one that has identical long-term averages but reduced day-to-day variability of meteorological variables, such as air temperature and precipitation. The differences in long-term average results from these two model runs will therefore demonstrate the exclusive effects of temporal vari-  
85 ability of climate variables and extreme meteorological events on MAGT in high latitude permafrost regions.

## 2 Methods

### 2.1 The land surface model JSBACH

The Jena Scheme for Biosphere-Atmosphere Coupling in Hamburg (JSBACH) is the land surface  
90 scheme for the Max Planck Institute Earth System Model (MPI-ESM) (Raddatz et al., 2007; Reick et al., 2013). It runs coupled to the atmosphere inside the ESM or offline forced by observation-based or projected climate input data. This model has recently been advanced by several processes which



are particularly important in cold regions (Ekici et al., 2014): coupling of soil hydrology and heat conduction via latent heat of fusion and the effects of soil ice and water content on thermal properties, and a snow model for soil insulation. The model simulates heat conduction and soil hydrology in a 1-D vertical scheme using several layers (Hagemann and Stacke, 2015). The version used in this study has been updated from the one used in Ekici et al. (2014) by two additional deep soil layers for thermal and hydrological processes of 13 and 30 m, respectively, which lead to a total potential soil profile of 53 m. However, soil hydrological processes are constrained by the depth to the bedrock. Another constraint on soil hydrological processes is the potentially available pore volume which is reduced by ice content.

In contrast to the model version described in Ekici et al. (2014), here we use a further advanced snow module that includes *dynamic* snow density and snow thermal properties (Ekici, 2015). In this approach, the snow density ( $\rho_{snow}$ ) follows a similar representation as in Verseghy (1991). It is initialized with a minimum value of  $\rho_{min} = 50 \text{ kg m}^{-3}$ . Then the compaction effect is included as a function of time and a maximum density ( $\rho_{max} = 300 \text{ kg m}^{-3}$ ) value (Eq. 1),

$$\rho_{snow}^{t+1} = (\rho_{snow}^t - \rho_{max}) \exp \frac{-0.002 \cdot \Delta t}{3600} + \rho_{max} \quad (1)$$

where  $\Delta t$  is the timestep length of model simulation. Additionally, when there is new snowfall, snow density is updated by taking a weighted average of fresh snow density ( $\rho_{min}$ ) and the calculated snow density value of the previous timestep.

Snow density controls snow heat conduction parameters. Eq. 2 and Eq. 3 show the relationships of volumetric snow heat capacity ( $c_{snow}$ ) and snow heat conductivity ( $\lambda_{snow}$ ) to snow density following the approach of Abels (1892) and Goodrich (1982). With no previous snow layers,  $c_{snow}$  is initialized with an average value of  $0.52 \text{ MJ m}^{-3} \text{ K}^{-1}$  and  $\lambda_{snow}$  with  $0.1 \text{ W m}^{-1} \text{ K}^{-1}$ ,

$$c_{snow} = c_{ice} \cdot \rho_{snow} \quad (2)$$

where  $c_{ice}$  is the specific heat capacity of ice ( $2106 \text{ J kg}^{-1} \text{ K}^{-1}$ ), and

$$\lambda_{snow} = 2.9 \cdot 10^{-6} \cdot (\rho_{snow})^2 \quad (3)$$

Another important advancement of the JSBACH model version used in this study is the inclusion of a dynamic lichen and bryophyte model (Porada et al., 2013, 2016a). This model is designed to predict lichen and bryophyte net primary productivity (NPP) in a process-based way from available light, surface temperature, atmospheric carbon dioxide concentration, and water content of lichens and bryophytes. Furthermore, it is applicable to estimate various impacts of lichens and bryophytes on biogeochemical cycles (Porada et al., 2016b; Lenton et al., 2016; Porada et al., 2017). The model includes a dynamic representation of the surface cover which depends on the balance of growth due to NPP and reduction by disturbance, such as fire (Porada et al., 2016a). The coverage of the layer determines its influence on heat exchange between atmosphere and soil. The layer thickness and porosity is set to 4.5 cm and 80%, respectively.



The lichen and bryophyte water balance is integrated into the scheme of hydrological fluxes in JSBACH. In addition, the lichen and bryophyte layer is fully integrated into the heat conduction  
130 scheme and hence also functions as a soil insulating layer (Porada et al., 2016a). Soil insulation depends on the fractional grid cell coverage of the lichen and bryophyte layer as well as on its hydrological status. Thereby, thermal diffusivity of this layer is computed as a function of water, ice and air content in the lichen and bryophyte layer (Porada et al., 2016a). The simulated relations between thermal properties of the lichen and bryophyte layer and water content agree well with  
135 field observations. Porada et al. (2016a) provide a complete description of the dynamic lichen and bryophyte model in JSBACH. The model version used here differs from Porada et al. (2016a) only with respect to the parametrisation of the snow layer, which has a slightly longer compression time, and a few bug fixes. This updated version is also used in Chadburn et al. (2017), where it shows good agreement with site level soil temperature observations.

## 140 2.2 Model experiments

For addressing the research question about effects of climate variability on mean annual ground temperature in permafrost regions (cf. section 1), artificial model experiments are conducted in this study. In addition to the control model run (CNTL), in one model experiment called REDVAR the land surface model has been driven by an artificial climate dataset that represents a reduced short-  
145 term (day-to-day) climate variability while the decadal averages are conserved (section 2.4). Then, differences in decadal averages of simulated snow and lichen and bryophyte properties and ultimately soil temperature can be interpreted exclusively due to a difference in variability of meteorological variables.

Two different kinds of such experiments are presented in this study. The main experiments are  
150 conducted at the pan-Arctic scale over historical to recent time periods (1901-2010). Here, CNTL and REDVAR model runs are done exactly the same way including the spin-up approach for reservoir initialization. At the end, results are compared from "two different worlds" with the same average climate, one with a constantly lower variability of meteorological variables than the other.

The second kind of experiments has been performed at site-level scale. Here, JSBACH has been  
155 run over the period 1901-2100 (CNTL) and a second model run with constantly *increasing* reduction of climate variability (REDVARfut, see section 2.4) has been performed for the period 2011-2100. This experiment additionally clarifies the effects of changing future climate variability on permafrost temperature. The REDVARfut experiment additionally contribute to the question on how climate data should be prepared in order to perform so called offline model experiments into the future.  
160 Of particular concern are potential biases in future projections of ecosystems states using LSMs because in these projections anomalies of raw ESM output is usually added to recent short-term variability of meteorological variables. Even if that is the most reliable approach of conducting such future projections at the moment, still we need to address the question, how high could be the bias



just because a change in short-term variability has been neglected? The REDVARfut experiment has  
165 been conducted for two grid cells representing two sites, one Canadian site at about 62.2N, -75.6E  
with MAGT of about -5 deg C, and one East Siberian site at about 72.2N, 147E with MAGT of about  
-10 deg C. At these sites, JSBACH results differed by only 0.7 and 0.2 deg C from these borehole  
measurements.

State variables have been brought into equilibrium using a spin-up approach prior to the transient  
170 model runs (1901-2010 or 1901-2100). We assume the time period 1901-1930 to be a representative  
for pre-industrial climatology following (Cramer et al., 1999; McGuire et al., 2001). Therefore,  
randomly selected years from that period have been used. For a proper spin-up of soil physical  
state variables in permafrost regions, we suggest a 2-step procedure. First, a 50-year model run with  
175 the above described randomly selected climate from the period 1901-1930 has been done without  
considering any freezing and thawing. This first spin-up will bring the soil temperature and water  
pools in a first equilibrium with pre-industrial climate. In a second step, another 100 years spin-up  
with the same climate data is performed but now freezing and thawing is switched on in order to  
have all pools including soil ice and water content, and soil temperature in equilibrium with climate.

### 2.3 Forcing data

180 The JSBACH model estimates half-hourly climate forcing data using daily data of maximum and  
minimum air temperature, precipitation, short-wave and long-wave radiation, specific humidity and  
surface pressure. We are using global data at 0.5 degree spatial resolution which has been produced  
following the description in (Beer et al., 2014). The historical data from 1901-1978 came from the  
WATCH forcing dataset (Weedon et al., 2011), and for the period 1979-2010 ECMWF ERA-Interim  
185 reanalysis data (Dee et al., 2011) has been bias-corrected against the WATCH forcing data following  
Piani et al. (2010) as described in Beer et al. (2014).

For a specific additional projection into the future (REDVARfut, section 2.2), meteorological data  
during 2011-2100 have been obtained from the CMIP5 output of the Max-Planck-Institute Earth  
System Model (Giorgetta et al., 2012) following the representative concentration pathway (RCP)  
190 8.5. Meteorological data of the two grid cells representing the Canadian and Russian sites were cut  
out and then also bias corrected to the observation-based period following Piani et al. (2010) as  
described in Beer et al. (2014).

Grid cells are divided into four tiles according to the four most dominant vascular plant func-  
tional types of this grid cell (Ekici et al., 2014). This vascular vegetation coverage is assumed to  
195 stay constant over the time of simulation. In the model simulations used in this study, we apply  
new soil parameters. Hydrological parameters have been assigned to each soil texture class follow-  
ing Hagemann and Stacke (2015) according to the percentage of sand, silt and clay at 1 km spatial  
resolution as indicated by the Harmonized World Soil Database (FAO/IIASA/ISRIC/ISSCAS/JRC,  
2012). Thermal parameters have been estimated as in (Ekici et al., 2014) at the 1 km spatial resolu-



200 tion. Then, averages of 0.5-degree grid cells have been calculated. Soil depth until bedrock follows  
the map used in Carvalhais et al. (2014) based on Webb et al. (2000).

#### 2.4 Meteorological forcing data with manipulated variability

Based on the climate data described above (subsequently called CNTL dataset), an additional cli-  
mate dataset has been developed. This dataset shows reduced day-to-day variability but conserved  
205 long-term mean values when comparing to CNTL, as described in detail in Beer et al. (2014). The  
dataset with reduced variability is called REDVAR. In that dataset, the variability of daily values is  
reduced by a variance factor of  $k = 0.25$  (see Beer et al. (2014) for details), but the mean seasonal cy-  
cle is conserved. The seasonal variability is represented by an 11-year running average across same  
dates. Differently from Beer et al. (2014), seasonal means in the REDVAR dataset were exactly pre-  
210 served by normalization with respect to the CNTL dataset for the annual quarters December-January-  
February, March-April-May, June-July-August, and September-October-November for each year in-  
dividually.

For the specific additional projection until 2100 at site-level scale, bias-corrected future climate  
data has been manipulated such that the short-term variability of meteorological variables *is dynam-*  
215 *ically* reducing during 2011-2100, in contrast to the REDVAR dataset for which a constant reduction  
factor has been applied. This additional artificial dataset is called REDVARfut in the following.  
For REDVARfut, the variance factor  $k$  is set to change linearly from 1 to 0.1 over these 90 years  
following Eq. 4:

$$k = 1 - (2.7^{-5} \cdot d) \quad (4)$$

220 where  $d$  is the day relative to 1 Jan 2011. This has been done for two grid cells representing one  
location in Canada (medium recent MAGT) and one location in East Siberia (cold recent MAGT)  
(cf. section 2.2). The CNTL and REDVARfut datasets are identical for the time period before 2011.

### 3 Mean annual ground temperature evaluation

The frost-enhanced JSBACH model has been intensively evaluated elsewhere (Ekici et al., 2014,  
225 2015; Porada et al., 2016a). The model version used here has also been recently extensively evalu-  
ated against site-level observations (Chadburn et al., 2017). In this paper, the simulated mean annual  
ground temperature (MAGT) is again evaluated against various other datasets at different spatial  
scales. First, JSBACH model results are compared to model results from the GIPL 1.3 model (Uni-  
versity of Alaska Fairbanks) over Alaska for the period 1980-1989. For this comparison we used  
230 JSBACH mean soil temperature results from layer 7 (38 m depth) and during 1980-1989. Then, spa-  
tial details of MAGT are compared to the information from the Geocryological Map of Yakutia (Beer  
et al., 2013) using also model results from layer 7 but a mean value during 1960-1989. The depth  
of 38 m ensures that temperature variation is negligible and hence comparable to the information in



the observation-based map. Last, JSBACH subsoil temperature is compared to pan-Arctic borehole  
235 measurements collected by the GTN-P initiative (Romanovsky et al., 2010; Christiansen et al., 2010;  
Smith et al., 2010) using model results from the layer corresponding to the measurement depth and  
from year 2008. The respective GTN-P Thermal State of Permafrost (TSP) snapshot data has been  
downloaded from the National Snow and Ice Data Center (NSIDC).

### 3.1 Analysis

240 In order to analyse effects of variability of meteorological variables on snow and near-surface veg-  
etation properties and hence soil temperature, model results have been averaged during the period  
1980-2009. As the averages of climate forcing data is similar between both experiments REDVAR  
and CNTL, (relative) differences in long-term average model results, such as snow depth or soil tem-  
perature, show the effects of short-term variability of climate forcing data. Relative differences are  
245 displayed as a fraction (no unit). In Fig. 4 to Fig. 9 the dark green area represents all land outside the  
(sporadic) permafrost zone which is masked by applying a long-term mean air temperature threshold  
of  $-3\text{ }^{\circ}\text{C}$ .

## 4 Results

### 4.1 Mean annual ground temperature evaluation

250 When comparing against a global dataset of mean annual ground temperature (MAGT) at depth  
ranging usually from 1 to 20 m (GTN-P initiative) JSBACH shows almost no bias ( $-0.4\text{ }^{\circ}\text{C}$ ) and  
a root mean square error of  $3\text{ }^{\circ}\text{C}$  Fig. 1. JSBACH represents the spatial variation in mean annual  
ground temperature (MAGT) reasonably well with a coefficient of determination of 0.5. Fig. 1 shows  
that for a number of measurements between  $0$  and  $-1\text{ }^{\circ}\text{C}$ , JSBACH simulates a larger variation  
255 ranging from  $2$  to  $-8\text{ }^{\circ}\text{C}$ . In addition, JSBACH clearly underestimates MAGT at three borehole  
sites in the Canadian High Arctic (data about  $-10\text{ }^{\circ}\text{C}$ , model about  $-22\text{ }^{\circ}\text{C}$ ) which requires further  
evaluation, e.g. about the representativeness of these data points or about the validity of snowfall  
input data to the model.

When looking at alternative estimates of spatial details of MAGT, JSBACH both underestimate  
260 or overestimate MAGT by about  $2$  to  $4\text{ }^{\circ}\text{C}$  depending on the location (Fig. 2, Fig. 3). The JSBACH  
results for Alaska are compared to another model output. JSBACH overestimates MAGT in many ar-  
eas in Alaska by several  $^{\circ}\text{C}$  while also underestimates MAGT at the southern end of the North Slope  
(Fig. 2). In East Siberia (Yakutia), the model usually underestimates MAGT by  $2$  to  $6\text{ }^{\circ}\text{C}$  (Fig. 3)  
when comparing to an observation-based map (Beer et al., 2013). However, the cold bias is largely  
265 reduced when taking the uncertainty (standard deviation) in the original geocryological map into ac-  
count (Fig. 3). Then, the difference is negligible in many regions. Still, there is a very strong cold bias  
in the mountainous regions of East Siberia. When taking the map uncertainty into account (Fig. 3)





the model still underestimates MAGT by about 6 to 8 °C here. This bias can also not be explained  
by the general warm bias of very low MAGT in the geocryological map when comparing to GTN-P  
270 observations (Beer et al., 2013). In fact, very low snow depth model results in these areas of about  
15 cm on average (data not shown) seem to be the reason for a too low insulation of soil during a  
very cold winter.

#### 4.2 Climate forcing data comparison

The long-term (1980-2010) averages of air temperature differ by only 0.015 °C at maximum or  
275 0.004 % between CNTL and REDVAR in permafrost regions (Fig. 4a). Also long-term precipitation  
averages are similar between the datasets, with differences of -0.2 to 0.1 % (Fig. 4b).

In contrast, the difference in short-term variability of meteorological variables at daily resolution  
between both datasets is remarkable. Although the statistical transformation of variables has been  
performed at residuals to the mean seasonal cycle (section 2.4), still the standard deviation of air  
280 temperature at daily resolution is usually 0.2 to 1 °C lower in the REDVAR dataset compared to  
CNTL, or 2 to 10 % (Fig. 5a). That means that temperature of warmer days have been reduced while  
air temperature of colder days have been increased such that the overall mean air temperature is  
similar. Interestingly, the amount of variability difference between the two datasets also depends on  
the location. For example, lower standard deviation differences are visible towards colder regions,  
285 such as East Siberia and the Canadian High Arctic. One explanation for this pattern is the higher  
mean seasonal cycle in continental climate, which has not been manipulated (section 2.4), and which  
therefore dominates stronger the overall variability, which is analyzed in Fig. 5a. Also REDVAR  
precipitation standard deviation is usually 2 to 6 % lower than precipitation standard deviation of the  
CNTL dataset (Fig. 5b). Hence, in this artificial climate dataset, extremely heavy rainfall or snowfall  
290 is reduced while small precipitation amounts have been increased.

#### 4.3 Climate variability effects on snow properties

Importantly, snow depth is up to 20 percent higher under reduced climate variability conditions  
(Fig. 6a). In fact, the snow depth difference can be explained by differences in snow water equivalents  
of same magnitude (Fig. 6b). In contrast, the slightly higher snow density under reduced climate  
295 variability (Fig. 6c) is not able to explain the difference in snow depth. Snow melt flux differences in  
autumn between both model experiments of 10 to 40 percent (Fig. 6d) demonstrate clearly that under  
reduced air temperature variability during the beginning of the snow season, individual snow melt  
events and hence the total snow melt flux are reduced. Besides snow depth, the thermal diffusivity  
of snow controls the overall heat conduction. Fig. 7 shows that under reduced climate variability  
300 conditions, thermal diffusivity of snow is 0.5 to 2.5 percent higher in high latitude regions.



#### 4.4 Climate variability effects on thermal diffusivity of lichens and bryophytes

Thermal diffusivity of lichens and bryophytes differs only marginally between the REDVAR and CNTL model experiments over most of the northern high latitude permafrost regions (Fig. 8a). In western Siberia and Quebec, winter moss thermal diffusivity is up to 12 percent lower under reduced  
305 climate variability conditions (Fig. 8a). In contrast, summer moss diffusivity is usually higher under reduced variability of meteorological variables (Fig. 8b). Under these climate conditions, it is raining more often a little bit and air temperature are not extreme resulting in more moist conditions for lichens and bryophytes, hence higher thermal diffusivity. In tundra the difference is about 2 percent while in the boreal forest it can be up to 6 percent (Fig. 8b).

#### 310 4.5 Ultimate climate variability effects on soil temperature

The estimated long-term average of both topsoil and subsoil temperature differs between REDVAR and CNTL experiments (Fig. 9a, Fig. 9b). Soil is 0.1 to 0.8 °C warmer when climate variability is reduced (Fig. 9a, Fig. 9b). These results and also the spatial pattern are similar between topsoil and subsoil values (Fig. 9a, Fig. 9b) with a bit larger effect on topsoil temperature. Soil temperature  
315 differences are larger in winter with values up to 1.5 °C compared to the summer when differences are typically 0.2-0.5 °C (Fig. 9c, Fig. 9d).

#### 4.6 Effects of future changes of climate variability on soil temperature

In order to analyze effects of changing variability of meteorological variables in time, the results of the respective additional model runs into the future at two sites are displayed as time series in  
320 Fig. 10 and Fig. 11. In contrast to the continental model experiments, in these additional point simulations the variability of meteorological variables is increasingly reduced during 2011-2100 in the REDVARfut input dataset while the historical climate until 2010 is identical (section 2.4).

The bias-corrected MPI-ESM CMIP5 model output following RCP8.5 shows increasing air temperature in both locations (solid blue line in Fig. 10a and Fig. 11a). Precipitation is also slightly increasing (solid blue line in Fig. 10b and Fig. 11b). This positive trend is also seen by the annual minimum (percentile 1) and maximum (percentile 99) temperature, and maximum precipitation (dashed blue lines in Fig. 10 and Fig. 11). Meteorological forcing data of the REDVARfut dataset (red lines) shows similar long-term averages to the CNTL dataset (Fig. 10a, Fig. 10b, Fig. 11a, Fig. 11b). Hence, REDVARfut variables follow the general positive trend. However, as the short-term variability is designed to be increasingly reduced, the differences in the minimum (1-percentile) and maximum (99-percentile) air temperature are increasing during 2011-2100. The increasing maximum daily precipitation in the CNTL dataset has been reversed in REDVARfut where the amount of precipitation at percentile 99 is even decreasing in time (Fig. 10b, Fig. 11b).



These CNTL and REDVARfut climate datasets have been used as forcing data for JSBACH in the  
335 additional point-scale model runs. The respective soil temperature results are compared to each other  
in Fig. 10 and Fig. 11. The time-varying changes in the variability of meteorological variables under  
conserved long-term average leads to a difference in topsoil temperature of up to 0.8 °C (Fig. 10c,  
Fig. 11c), i.e. the overall increasing topsoil temperature due to increasing air temperature is a bit  
higher in case of reduced climate variability. This effect is also visible in 38 m depth (Fig. 10d,  
340 Fig. 11d) even though short-term atmospheric data fluctuations should be most filtered at this depth.

## 5 Discussion

Climate model projections show increasing variability of meteorological variables and hence in-  
creasing frequency of extreme meteorological events (Seneviratne et al., 2012) along with a gradu-  
ally changing climate (change of long-term mean values) (Ciais et al., 2013). Because of the non-  
345 linearity of ecosystem response functions, changing extreme event frequency and changing variabil-  
ity of meteorological variables can have a higher impact on ecosystem state and function than a  
gradual change of mean meteorological variables (Reichstein et al., 2013; Beer et al., 2014). This  
study contributes to this overall question from a theoretical point of view with LSM experiments for  
which artificially manipulated climate forcing datasets have been employed. These climate datasets  
350 practically do not differ in their decadal averages (section 4.2) while they are showing a substan-  
tial difference in the short-term (daily) variability (section 4.2). Therefore, differences in simulated  
state variables and fluxes over 30-year periods (soil temperature in this case) will be only due to  
differences in *temporal variability* of meteorological variables. This study addresses particularly the  
question about the effect of climate variability on soil temperature in northern high latitude regions.  
355 The CNTL experiment shows *higher* climate variability than the artificial experimental REDVAR  
dataset (sections 2.4 and 4.2), and respective model result differences between experiments using  
the manipulated climate REDVAR) and the CNTL dataset are shown in section 4. Methodologi-  
cally, it is important to artificially design a climate dataset with *reduced* temporal variability because  
otherwise there is a high risk for producing a physically unrealistic climate conditions. However,  
360 for interpreting the results in terms of future ecosystem responses to *increasing* climate variability  
(Seneviratne et al., 2012), **the direction of the conclusions are carefully inverted in this discus-  
sion section.**

In contrast to the climate forcing data, the long-term average of both topsoil and subsoil tem-  
perature differs between REDVAR and CNTL experiments (Fig. 9a, Fig. 9b). The same is true for  
365 respective future projections (Fig. 10, Fig. 11). In fact, under higher variability of meteorological  
variables and higher frequency of extreme events (CNTL versus REDVAR experiments) soil will be  
cooler (Fig. 9c, Fig. 9d, Fig. 10, Fig. 11) given all other environmental factors are similar. That means  
that the projected increase in future variability of meteorological variables (Seneviratne et al., 2012)



has the potential to dampen soil warming occurring as a function of increasing mean air temperature.  
370 To further understand the underlying processes, individual effects of climate variability on snow and near-surface vegetation properties are discussed in the following paragraphs.

For land-atmosphere heat conduction the thermal properties of snow, near-surface vegetation (e.g. mosses and lichens), the soil organic layer, and their spatial extent and heights are of major importance (Yershov, 1998; Gouttevin et al., 2012; Wang et al., 2016; Jafarov and Schaefer,  
375 2016). Snow generally insulates the soil from changing atmospheric temperature. However, effects are smaller during the melting period in spring because the snow is wet and conductivity therefore higher, and more importantly, the soil-to-air gradient in temperature is small. The insulation effect of near-surface vegetation also differs among the seasons because of the high dependence of thermal properties on water and ice contents of lichens and bryophytes. Usually, dry lichens and bryophytes  
380 during a continental summer should insulate much more than during wet spring or autumn, or during the ice-rich winter time.

This theoretical study shows that one major effect of higher climate variability on cold region environments is a lower snow water equivalent (section 4.3) which directly translates into lower snow depth values. The potential alternative explanation for a lower snow depth would be a higher snow  
385 density. However, the results show exactly the opposite (Fig. 6c). In addition to snow depth, snow thermal properties are also an important factor for heat conduction. However, winter snow thermal diffusivity is some percent lower under higher climate variability conditions (CNTL-REDVAR). Therefore, the net *snow-related* effect of higher climate variability on soil temperature, that is a cooler soil (section 4.5) is explained by snow depth differences alone, i.e. a lower snow depth under  
390 higher climate variability.

The reason for these snow water equivalent differences are more often circumstances of melting snow during the beginning of the snow season when day-to-day variability of air temperature is higher (section 4.3). These results also point to an interesting combination of impacts of both changing variability *and* gradually changing mean values on ecosystem states because both changes can  
395 lead to pass a threshold value (melting point in this case). These impacts can be seen in section 4.3 when combining temporal climate variability effects on snow water equivalent results (Fig. 6) and snow melt flux results (Fig. 6d) with longitudinal pattern of these results towards a continental climate, which can be interpreted in terms of gradual climate change when substituting space for time. Overall, these findings show that projected higher climate variability in future can lead to lower snow  
400 depth which will reduce a soil warming in response to air warming.

In addition to the insulating effect of snow, lichens and bryophytes growing on the ground influence on heat conduction (Porada et al., 2016a). It is interesting to note that when climate variability is higher (CNTL conditions), moss thermal diffusivity can be substantially *higher in winter* and *lower in summer* in the same region (section 4.4). This fact points to an important role of near-surface  
405 vegetation: it will insulate less from air temperature during winter and insulate more during summer



with increasing climate variability in future. These effects of climate variability on thermal diffusivity of lichens and bryophytes and hence soil temperature are in the same direction as snow effects (section 4.3), again reducing the soil warming effect of future climate change.

Effects of climate variability on both snow and moss properties are in the same direction (sections 410 4.3 and 4.4). As a result, soil will be cooler under higher climate variability (section 4.5). Recent modelling studies suggest a soil temperature increase of 0.02 °C per year since 1960 (McGuire et al., 2016) which translates into 2 °C in 100 years. Such soil temperature increase has also been projected using the JSBACH model under the RCP4.5 scenario (Ekici, 2015) while under the strong warming scenario RCP8.5, the soil temperature increase might be up to 6 to 8 °C (Ekici, 2015). Lower soil 415 temperature under higher climate variability in the range 0.1 to 0.8 °C (section 4.5) demonstrate that under increasing variability of meteorological variables and increasing extreme events in the Arctic (Seneviratne et al., 2012), the effect of gradual air temperature increase on soil temperature and hence active-layer thickness will be *dampened*. Such dampening of future soil warming will also reduce the otherwise positive biogeochemical feedback to climate (Zimov et al., 2006; Beer, 2008; Heimann 420 and Reichstein, 2008). Our results are conservative here because the 99 percentiles of air temperature and precipitation from the artificial dataset (REDVAR) differ by only 1-4 °C (temperature) and 1-10 % (precipitation). These values are at the lower end of the range of climate model projections for the Arctic region until 2100 (Seneviratne et al., 2012).

The presented effects of short-term variability of meteorological variables on ecosystem states 425 and functions, such as soil temperature, are also important from a methodological point of view. To study the effects of environmental change on ecosystems, LSMs are usually forced by historical and reanalysis climate data for the past and present periods, and by future climate results from Earth system models. Since ESM results usually show biases, the ESM outputs cannot be used directly to drive the LSM offline model runs but first need to be bias-corrected (Hempel et al., 430 2013). The results of the presented REDVAR and REDVARfut experiments demonstrate that such bias-correction methods should account for the projected change in short-term (daily) variability in addition to general trends.

In addition, a first run of the MPI-ESM with the permafrost-advanced land surface scheme JSBACH coupled to the atmosphere model showed a remarkable bias in 2m air temperature of 1-4 435 °C in permafrost regions compared to the standard model version without freezing and thawing (Hagemann et al., 2016). Our results suggest that this bias could be potentially reduced when implementing representations of dynamic snow and of dynamic lichens and bryophytes.

Our findings have three major implications for future permafrost science:

1. New highly controlled laboratory and field experiments are required in order to confirm modelling results about climate variability effects on permafrost soil temperature. 440
2. Future developments of land surface models should include dynamic models of snow, and lichens and bryophytes.



3. Statistical methods need to be developed such that future forcing data for climate change  
impact studies can be prepared in a way that a potential change in short-term variability and  
445 frequency of extreme events is preserved.

## 6 Conclusions

Artificial model experiments have been used in order to quantify the impact of the variability of  
meteorological variables on the long-term mean of mean annual ground temperature in permafrost-  
affected terrestrial ecosystems. This impact is mainly due to temperature variability effects on snow  
450 melt and snow depth as well as climate variability effects on the (seasonally different) thermal dif-  
fusivity of lichens and bryophytes. Overall, the soil temperature response to increasing climate vari-  
ability and extreme event frequency (soil cooling) will be opposite to the response of soil temperature  
to gradually increasing air temperature (soil warming). This shows the importance of representing  
dynamically snow and lichen and bryophyte functions in Earth system models for projecting fu-  
455 ture permafrost soil states and land-atmosphere interactions, hence future climate. Our findings also  
point to the need to represent changes in short-term variability of meteorological variables in bias-  
corrected climate data of future periods.

*Acknowledgements.* Financial support came from the European Union FP7-ENV project PAGE21 under con-  
tract number GA282700. Model simulations were performed on resources provided by the Swedish National  
460 Infrastructure for Computing (SNIC) at Linköping University. We acknowledge the Land Department, Max  
Planck Institute for Meteorology, Hamburg, Germany for JSBACH code maintenance. We thank Charles Koven  
for a constructive review that helped to improve a previous version of the manuscript. We further acknowledge  
the borehole temperature dataset "IPA-IPY Thermal State of Permafrost (TSP) Snapshot Borehole Inventory,  
Version 1.0" downloaded from NSIDC.



## 465 References

- Abels, H.: Beobachtungen der täglichen Periode der Temperatur im Schnee und Bestimmung des Wärmeleitungsvermögens des Schnees als Funktion seiner Dichtigkeit, *Repertorium für Meteorologie*, 16, 1–53, 1892.
- Arrhenius, S.: Über die Reaktionsgeschwindigkeit bei der Inversion von Rohrzucker durch Säuren, *Z. Phys. Chem.*, 4, 226–248, 1889.
- 470 Beer, C.: Soil science: The Arctic carbon count, *Nature Geoscience*, 1, 569–570, <http://www.nature.com/ngeo/journal/v1/n9/abs/ngeo292.html>, 2008.
- Beer, C., Fedorov, A. N., and Torgovkin, Y.: Permafrost temperature and active-layer thickness of Yakutia with 0.5-degree spatial resolution for model evaluation, *Earth System Science Data*, 5, 305–310, doi:10.5194/essd-5-305-2013, <http://www.earth-syst-sci-data.net/5/305/2013/>, 2013.
- 475 Beer, C., Weber, U., Tomelleri, E., Carvalhais, N., Mahecha, M. D., and Reichstein, M.: Harmonized European Long-Term Climate Data for Assessing the Effect of Changing Temporal Variability on Land-Atmosphere CO<sub>2</sub> Fluxes, *Journal of Climate*, 27, 4815–4834, doi:10.1175/JCLI-D-13-00543.1, <http://journals.ametsoc.org/doi/pdf/10.1175/JCLI-D-13-00543.1>, 2014.
- 480 Callaghan, T. V., Bergholm, F., Christensen, T. R., Jonasson, C., Kokfelt, U., and Johansson, M.: A new climate era in the sub-Arctic: Accelerating climate changes and multiple impacts, *Geophys. Res. Lett.*, 37, L14 705, doi:10.1029/2009GL042064, 2010.
- Campbell, G. S. and Norman, J. M.: *An introduction to environmental biophysics*, Springer, New York, 2. ed. edn., 1998.
- 485 Carvalhais, N., Forkel, M., Khomik, M., Bellarby, J., Jung, M., Migliavacca, M., ?u, M., Saatchi, S., Santoro, M., Thurner, M., Weber, U., Ahrens, B., Beer, C., Cescatti, A., Randerson, J., and Reichstein, M.: Global covariation of carbon turnover times with climate in terrestrial ecosystems, *Nature*, 514, 213–217, doi:10.1038/nature13731, <http://www.nature.com/nature/journal/v514/n7521/full/nature13731.html>, 2014.
- Chadburn, S., Krinner, G., Porada, P., Bartsch, A., Beer, C., Beletti Marchesini, L., Boike, J., Elberling, B., 490 Friborg, T., Hugelius, G., Johansson, M., Kuhry, P., Kutzbach, L., Langer, M., Lund, M., Parmentier, F.-J., Peng, S., Van Huissteden, K., Wang, T., Westermann, S., Zhu, D., and Burke, E.: Carbon stocks and fluxes in the high latitudes: Using site-level data to evaluate Earth system models, *Biogeosciences Discussions*, 2017, 1–41, doi:10.5194/bg-2017-197, <http://www.biogeosciences-discuss.net/bg-2017-197/>, 2017.
- Christiansen, H. H., Etzelmüller, B., Isaksen, K., Juliussen, H., Farbrot, H., Humlum, O., Johansson, M., 495 Ingeman-Nielsen, T., Kristensen, L., Hjort, J., Holmlund, P., Sannel, A. B. K., Sigsgaard, C., Åkerman, H. J., Foged, N., Blikra, L. H., Pernošky, M. A., and Ødegård, R. S.: The thermal state of permafrost in the nordic area during the international polar year 2007-2009, *Permafrost and Periglacial Processes*, 21, 156–181, doi:10.1002/ppp.687, <http://dx.doi.org/10.1002/ppp.687>, 2010.
- Ciais, P., Sabine, C., Bala, G., Bopp, L., Brovkin, V., Canadell, J., Chhabra, A., DeFries, R., Galloway, J., 500 Heimann, M., Jones, C., Le Quéré, C., Myneni, R., Piao, S., and Thornton, P.: Carbon and Other Biogeochemical Cycles, in: *Climate change 2013: The Physical Science Basis. Contribution of Working Group I to the Fifth Assessment Report of the Intergovernmental Panel on Climate Change*, pp. 465–570, Cambridge University Press, Cambridge, United Kingdom and New York, NY, USA, 2013.



- Cramer, W., Kicklighter, D., Bondeau, A., Iii, B. M., Churkina, G., Nemry, B., Ruimy, A., Schloss, A., et al.:  
505 Comparing global models of terrestrial net primary productivity (NPP): overview and key results, *Global  
Change Biology*, 5, 1–15, <http://onlinelibrary.wiley.com/doi/10.1046/j.1365-2486.1999.00009.x/full>, 1999.
- Dee, D., Uppala, S., Simmons, A., Berrisford, P., Poli, P., Kobayashi, S., Andrae, U., Balmaseda, M., Balsamo,  
G., Bauer, P., et al.: The ERA-Interim reanalysis: configuration and performance of the data assimilation  
system, *Quarterly Journal of the Royal Meteorological Society*, 137, 553–597, <http://onlinelibrary.wiley.com/doi/10.1002/qj.828/full>, 2011.
- 510 Easterling, D., Meehl, G., Parmesan, C., Changnon, S., Karl, T., and Mearns, L.: Climate Extremes: Observa-  
tions, Modeling, and Impacts, *Science*, 289, 2068–2074, 2000.
- Ekici, A.: Process-oriented representation of permafrost soil thermal dynamics in Earth System Models, Dis-  
sertation, University Fribourg, 2015.
- 515 Ekici, A., Beer, C., Hagemann, S., Boike, J., Langer, M., and Hauck, C.: Simulating high-latitude permafrost  
regions by the JSBACH terrestrial ecosystem model, *Geosci. Model Dev.*, 7, 631–647, doi:10.5194/gmd-7-  
631-2014, <http://dx.doi.org/10.5194/gmd-7-631-2014>, 2014.
- Ekici, A., Chadburn, S., Chaudhary, N., Hajdu, L. H., Marmy, A., Peng, S., Boike, J., Burke, E., Friend, A. D.,  
Hauck, C., Krinner, G., Langer, M., Miller, P. A., and Beer, C.: Site-level model intercomparison of high  
520 latitude and high altitude soil thermal dynamics in tundra and barren landscapes, *The Cryosphere*, 9, 1343–  
1361, doi:10.5194/tc-9-1343-2015, <http://www.the-cryosphere.net/9/1343/2015/>, 2015.
- FAO/IIASA/ISRIC/ISSCAS/JRC: Harmonized World Soil Database (version 1.2), FAO, Rome, Italy and  
IIASA, Laxenburg, Austria, 2012.
- Giorgetta, M., Jungclaus, J., Reick, C., Legutke, S., Brovkin, V., Crueger, T., Esch, M., Fieg, K., Glushak,  
525 K., Gayler, V., Haak, H., Hollweg, H.-D., Kinne, S., Kornblueh, L., Matei, D., Mauritsen, T., Mikolajew-  
icz, U., Müller, W., Notz, D., Raddatz, T., Rast, S., Roeckner, E., Salzmann, M., Schmidt, H., Schnur, R.,  
Segschneider, J., Six, K., Stockhause, M., Wegner, J., Widmann, H., Wieners, K.-H., Claussen, M., Marotzke,  
J., and Stevens, B.: CMIP5 simulations of the Max Planck Institute for Meteorology (MPI-M) based on  
the MPI-ESM-LR model: The rcp85 experiment, served by ESGF, doi:10.1594/WDCC/CMIP5.MXELr8,  
530 <https://doi.org/10.1594/WDCC/CMIP5.MXELr8>, 2012.
- Goodrich, L. E.: The influence of snow cover on the ground thermal regime, *Canadian Geotechnical Journal*,  
19, 421–432, 1982.
- Gouttevin, I., Menegoz, M., Dominé, F., Krinner, G., Koven, C., Ciais, P., Tarnocai, C., and Boike, J.: How  
the insulating properties of snow affect soil carbon distribution in the continental pan-Arctic area, *Jour-  
535 nal of Geophysical Research: Biogeosciences*, 117, doi:10.1029/2011JG001916, [http://dx.doi.org/10.1029/  
2011JG001916](http://dx.doi.org/10.1029/2011JG001916), g02020, 2012.
- Hagemann, S. and Stacke, T.: Impact of the soil hydrology scheme on simulated soil moisture memory, *Climate  
Dynamics*, 44, 1731–1750, <http://link.springer.com/article/10.1007%2Fs00382-014-2221-6>, 2015.
- Hagemann, S., Blome, T., Ekici, A., and Beer, C.: Soil-frost-enabled soil-moisture–precipitation feedback  
540 over northern high latitudes, *Earth System Dynamics*, 7, 611–625, doi:10.5194/esd-7-611-2016, [http://www.  
earth-syst-dynam.net/7/611/2016/](http://www.earth-syst-dynam.net/7/611/2016/), 2016.
- Heimann, M. and Reichstein, M.: Terrestrial ecosystem carbon dynamics and climate feedbacks, *Nature*, 451,  
289–292, 2008.





- Hempel, S., Frieler, K., Warszawski, L., Schewe, J., and Piontek, F.: A trend-preserving bias correction  
545 &ndash; the ISI-MIP approach, *Earth System Dynamics*, 4, 219–236, doi:10.5194/esd-4-219-2013, <http://www.earth-syst-dynam.net/4/219/2013/>, 2013.
- Jafarov, E. and Schaefer, K.: The importance of a surface organic layer in simulating permafrost thermal and  
carbon dynamics, *The Cryosphere*, 10, 465–475, doi:10.5194/tc-10-465-2016, <http://www.the-cryosphere.net/10/465/2016/>, 2016.
- 550 Koven, C. D., Ringeval, B., Friedlingstein, P., Ciais, P., Cadule, P., Khvorostyanov, D., Krinner, G., and  
Tarnocai, C.: Permafrost carbon-climate feedbacks accelerate global warming, *Proceedings of the National  
Academy of Sciences*, 108, 14 769–14 774, <http://www.pnas.org/content/108/36/14769.short>, 2011.
- Koven, C. D., Lawrence, D. M., and Riley, W. J.: Permafrost carbon-climate feedback is sensitive to deep soil  
carbon decomposability but not deep soil nitrogen dynamics, *Proceedings of the National Academy of Sci-*  
555 *ences*, 112, 3752–3757, doi:10.1073/pnas.1415123112, <http://www.pnas.org/content/112/12/3752.abstract>,  
2015.
- Lawrence, D. M., Slater, A. G., and Swenson, S. C.: Simulation of Present-Day and Future Permafrost and  
Seasonally Frozen Ground Conditions in CCSM4, *Journal of Climate*, 25, 2207–2225, doi:10.1175/JCLI-D-  
11-00334.1, <http://dx.doi.org/10.1175/JCLI-D-11-00334.1>, 2012.
- 560 Lenton, T. M., Dahl, T. W., Daines, S. J., Mills, B. J. W., Ozaki, K., Saltzman, M. R., and Porada, P.: Earliest  
land plants created modern levels of atmospheric oxygen, *Proceedings of the National Academy of Sciences*,  
113, 9704–9709, doi:10.1073/pnas.1604787113, <http://www.pnas.org/content/113/35/9704.abstract>, 2016.
- Lloyd, J. and Taylor, J. A.: On the temperature dependence of soil respiration, *Functional Ecology*, 8, 315–323,  
1994.
- 565 McGuire, A. D., Sitch, S., Clein, J. S., Dargaville, R., Esser, G., Foley, J., Heimann, M., Joos, F., Ka-  
plan, J., Kicklighter, D. W., Meier, R. A., Melillo, J. M., Moore, B., Prentice, I. C., Ramankutty, N., Re-  
ichenau, T., Schloss, A., Tian, H., Williams, L. J., and Wittenberg, U.: Carbon balance of the terrestrial  
biosphere in the Twentieth Century: Analyses of CO<sub>2</sub>, climate and land use effects with four process-  
based ecosystem models, *Global Biogeochemical Cycles*, 15, 183–206, doi:10.1029/2000GB001298, <http://dx.doi.org/10.1029/2000GB001298>,  
570 <http://dx.doi.org/10.1029/2000GB001298>, 2001.
- McGuire, A. D., Koven, C., Lawrence, D. M., Clein, J. S., Xia, J., Beer, C., Burke, E., Chen, G., Chen, X.,  
Delire, C., Jafarov, E., MacDougall, A. H., Marchenko, S., Nicolsky, D., Peng, S., Rinke, A., Saito, K., Zhang,  
W., Alkama, R., Bohn, T. J., Ciais, P., Decharme, B., Ekici, A., Gouttevin, I., Hajima, T., Hayes, D. J., Ji, D.,  
Krinner, G., Lettenmaier, D. P., Luo, Y., Miller, P. A., Moore, J. C., Romanovsky, V., Schädel, C., Schaefer,  
575 K., Schuur, E. A., Smith, B., Sueyoshi, T., and Zhuang, Q.: Variability in the sensitivity among model simu-  
lations of permafrost and carbon dynamics in the permafrost region between 1960 and 2009, *Global Biogeo-  
chemical Cycles*, 30, 1015–1037, doi:10.1002/2016GB005405, <http://dx.doi.org/10.1002/2016GB005405>,  
2016GB005405, 2016.
- Peng, S., Ciais, P., Krinner, G., Wang, T., Gouttevin, I., McGuire, A. D., Lawrence, D., Burke, E., Chen, X.,  
580 Decharme, B., Koven, C., MacDougall, A., Rinke, A., Saito, K., Zhang, W., Alkama, R., Bohn, T. J., Delire,  
C., Hajima, T., Ji, D., Lettenmaier, D. P., Miller, P. A., Moore, J. C., Smith, B., and Sueyoshi, T.: Simulated  
high-latitude soil thermal dynamics during



- the past 4 decades, *The Cryosphere*, 10, 179–192, doi:10.5194/tc-10-179-2016, <http://www.the-cryosphere.net/10/179/2016/>, 2016.
- 585 Piani, C., Weedon, G., Best, M., Gomes, S., Viterbo, P., Hagemann, S., and Haerter, J.: Statistical bias correction of global simulated daily precipitation and temperature for the application of hydrological models, *Journal of Hydrology*, 395, 199–215, <http://www.sciencedirect.com/science/article/pii/S0022169410006475>, 2010.
- Porada, P., Weber, B., Elbert, W., Pöschl, U., and Kleidon, A.: Estimating global carbon uptake by lichens and bryophytes with a process-based model, *Biogeosciences*, 10, 6989–7033, doi:10.5194/bg-10-6989-2013, 590 <http://www.biogeosciences.net/10/6989/2013/>, 2013.
- Porada, P., Ekici, A., and Beer, C.: Effects of bryophyte and lichen cover on permafrost soil temperature at large scale, *The Cryosphere*, 10, 2291–2315, doi:10.5194/tc-10-2291-2016, <http://www.the-cryosphere.net/10/2291/2016/>, 2016a.
- Porada, P., Lenton, T. M., Pohl, A., Weber, B., Mander, L., Donnadieu, Y., Beer, C., Poeschl, U., and Kleidon, 595 A.: High potential for weathering and climate effects of non-vascular vegetation in the Late Ordovician, *NATURE COMMUNICATIONS*, 7:12113, doi:10.1038/ncomms12113, 2016b.
- Porada, P., Pöschl, U., Kleidon, A., Beer, C., and Weber, B.: Estimating global nitrous oxide emissions by lichens and bryophytes with a process-based productivity model, *Biogeosciences*, 14, 1593–1602, doi:10.5194/bg-14-1593-2017, <http://www.biogeosciences.net/14/1593/2017/>, 2017.
- 600 Raddatz, T., Reick, C., Knorr, W., Kattge, J., Roeckner, E., Schnur, R., Schnitzler, K.-G., Wetzell, P., and Jungclaus, J.: Will the tropical land biosphere dominate the climate–carbon cycle feedback during the twenty-first century?, *Climate Dynamics*, 29, 565–574, <http://link.springer.com/article/10.1007/s00382-007-0247-8>, 2007.
- Rahmstorf, S. and Coumou, D.: Increase of extreme events in a warming world, *PNAS*, 108, 17 905–17 909, 605 doi:10.1073/pnas.1101766108, 2011.
- Reichstein, M., Bahn, M., Ciais, P., Frank, D., Mahecha, M. D., Seneviratne, S. I., Zscheischler, J., Beer, C., Buchmann, N., Frank, D. C., Papale, D., Rammig, A., Smith, P., Thonicke, K., van der Velde, M., Vicca, S., Walz, A., and Wattenbach, M.: Climate extremes and the carbon cycle, *Nature*, 500, 287–295, doi:10.1038/nature12350, <http://dx.doi.org/10.1038/nature12350>, 2013.
- 610 Reick, C. H., Raddatz, T., Brovkin, V., and Gayler, V.: Representation of natural and anthropogenic land cover change in MPI-ESM, *Journal of Advances in Modeling Earth Systems*, 5, 459–482, doi:10.1002/jame.20022, <http://dx.doi.org/10.1002/jame.20022>, 2013.
- Romanovsky, V., Smith, S., and Christiansen, H.: Permafrost thermal state in the polar Northern Hemisphere during the international polar year 2007–2009: A synthesis, *Permafrost and Periglacial Processes*, 21, 106– 615 116, <http://onlinelibrary.wiley.com/doi/10.1002/ppp.689/full>, 2010.
- Schaefer, K., Zhang, T., Bruhwiler, L., and Barrett, A. P.: Amount and timing of permafrost carbon release in response to climate warming, *Tellus B*, 63, 165–180, 2011.
- Schaphoff, S., Heyder, U., Ostberg, S., Gerten, D., Heinke, J., and Lucht, W.: Contribution of permafrost soils to the global carbon budget, *Environmental Research Letters*, 8, 014 026, <http://iopscience.iop.org/1748-9326/8/1/014026>, 2013. 620
- Schwalm, C. R., Anderegg, W. R. L., Michalak, A. M., Fisher, J. B., Biondi, F., Koch, G., Litvak, M., Ogle, K., Shaw, J. D., Wolf, A., Huntzinger, D. N., Schaefer, K., Cook, R., Wei, Y., Fang, Y., Hayes, D., Huang, M.,



- Jain, A., and Tian, H.: Global patterns of drought recovery, *Nature*, 548, 202–205, <http://dx.doi.org/10.1038/nature23021>, 2017.
- 625 Seneviratne, S., Nicholls, N., Easterling, D., Goodess, C., Kanae, S., Kossin, J., Luo, Y., Marengo, J., McInnes, K., Rahimi, M., Reichstein, M., Sorteberg, A., Vera, C., , and Zhang, X.: Changes in climate extremes and their impacts on the natural physical environment, in: *Managing the Risks of Extreme Events and Disasters to Advance Climate Change Adaptation*, edited by Field, C., Barros, V., Stocker, T., Qin, D., Dokken, D., Ebi, K., Mastrandrea, M., Mach, K., Plattner, G., Allen, S., Tignor, M., and Midgley, P., pp. 109–230, A Special Report of Working Groups I and II of the Intergovernmental Panel on Climate Change (IPCC). Cambridge University Press, Cambridge, UK, and New York, NY, USA, 2012.
- 630 Smith, S., Romanovsky, V., Lewkowicz, A., Burn, C., Allard, M., Clow, G., Yoshikawa, K., and Throop, J.: Thermal state of permafrost in North America: a contribution to the international polar year, *Permafrost and Periglacial Processes*, 21, 117–135, doi:10.1002/ppp.690, <http://dx.doi.org/10.1002/ppp.690>, 2010.
- 635 van't Hoff, J. H.: *Studien zur chemischen Dynamik*, W. Engelmann, Leipzig, 1896.
- Verseghy, D. L.: Class-A Canadian land surface scheme for GCMS. I. Soil model, *International Journal of Climatology*, 11, 111–133, doi:10.1002/joc.3370110202, <http://dx.doi.org/10.1002/joc.3370110202>, 1991.
- Wang, W., Rinke, A., Moore, J. C., Ji, D., Cui, X., Peng, S., Lawrence, D. M., McGuire, A. D., Burke, E. J., Chen, X., Decharme, B., Koven, C., MacDougall, A., Saito, K., Zhang, W., Alkama, R., Bohn, T. J., Ciais, P., Delire, C., Gouttevin, I., Hajima, T., Krinner, G., Lettenmaier, D. P., Miller, P. A., Smith, B., Sueyoshi, T., and Sherstiukov, A. B.: Evaluation of air–soil temperature relationships simulated by land surface models during winter across the permafrost region, *The Cryosphere*, 10, 1721–1737, doi:10.5194/tc-10-1721-2016, <http://www.the-cryosphere.net/10/1721/2016/>, 2016.
- Webb, R. W., Rosenzweig, C. E., and Levine, E. R.: Global Soil Texture and Derived Water-Holding Capacities (Webb et al.), doi:10.3334/ORNLDAAAC/548, <https://doi.org/10.3334/ORNLDAAAC/548>, 2000.
- 645 Weedon, G., Gomes, S., Viterbo, P., Shuttleworth, W., Blyth, E., Österle, H., Adam, J., Bellouin, N., Boucher, O., and Best, M.: Creation of the WATCH Forcing Data and its use to assess global and regional reference crop evaporation over land during the twentieth century, *Journal of Hydrometeorology*, 12, 823–848, <http://journals.ametsoc.org/doi/abs/10.1175/2011JHM1369.1>, 2011.
- 650 Wipf, S. and Rixen, C.: A review of snow manipulation experiments in Arctic and alpine tundra ecosystems, *Polar Research*, 29, 95–109, doi:10.1111/j.1751-8369.2010.00153.x, 2010.
- Yershov, E. D.: *General geocryology*, Cambridge University Press, Cambridge, UK., 1998.
- Zhang, T.: Influence of the seasonal snow cover on the ground thermal regime: An overview, *Reviews of Geophysics*, 43, n/a–n/a, doi:10.1029/2004RG000157, <http://dx.doi.org/10.1029/2004RG000157>, rG4002, 2005.
- 655 Zimov, S. A., Schuur, E. A. G., and Chapin, 3rd, F. S.: Climate change. Permafrost and the global carbon budget., *Science*, 312, 1612–1613, doi:10.1126/science.1128908, <http://dx.doi.org/10.1126/science.1128908>, 2006.

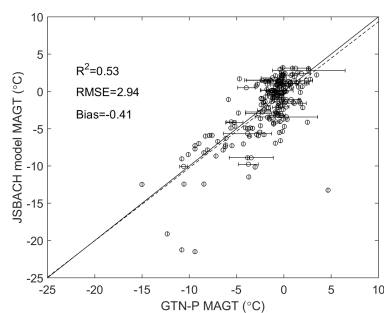


Figure 1: Evaluation of mean annual ground temperature against GTN-P borehole measurements.

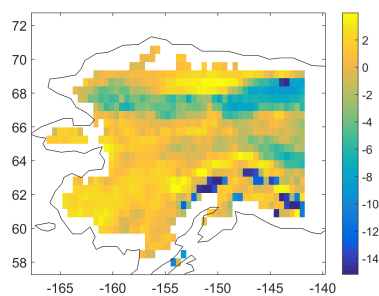


Figure 2: Difference in subsoil temperature ( $^{\circ}\text{C}$ ) between the models JSBACH and GIPL1.3 from the University of Alaska Fairbanks (1980-1989 average). JSBACH results from 49.5 m depth.

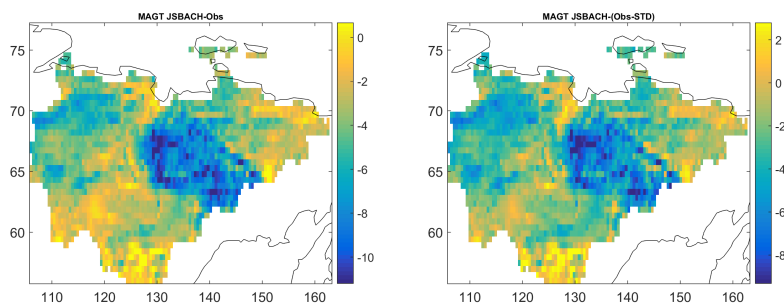


Figure 3: Difference in subsoil temperature ( $^{\circ}\text{C}$ ) between the JSBACH model (1960-1990 average) and the geocryological map of Yakutia (Beer et al., 2013). JSBACH results from 49.5 m depth. The right-hand side figure shows the difference to MAGT mean minus standard deviation from the geocryological map of Yakutia.

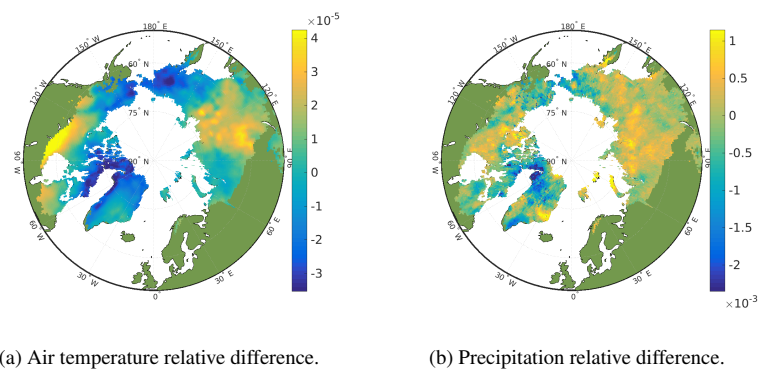


Figure 4: Comparison of 1980-2009 averages of meteorological variables (REDVAR versus CNTL).

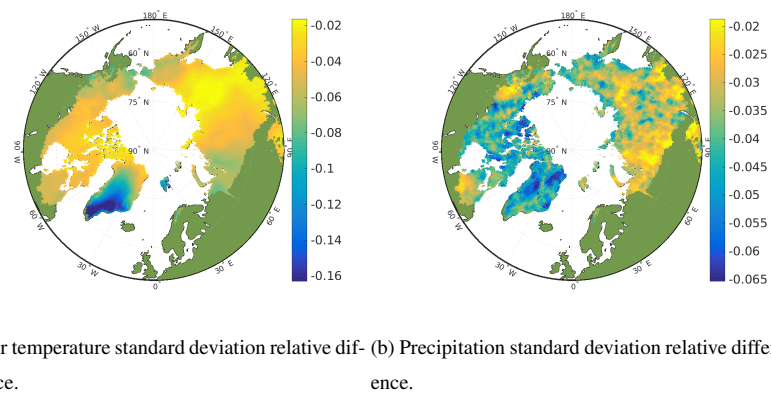


Figure 5: Comparison of 1980-2009 standard deviations of meteorological variables (REDVAR versus CNTL).

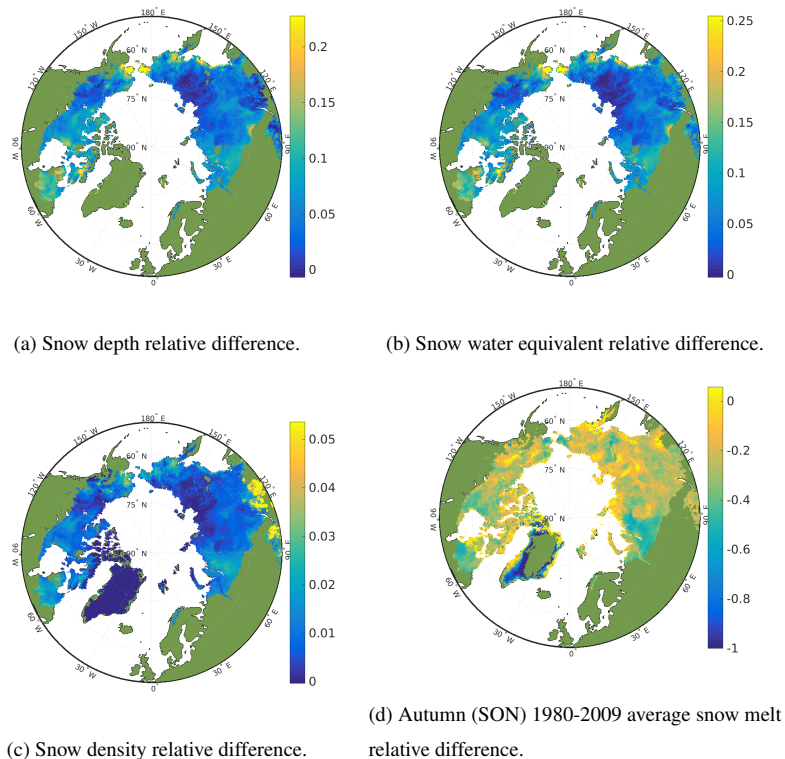


Figure 6: Comparison of mean winter (DJF) season snow properties during 1980-2009 (REDVAR versus CNTL). Numbers are expressed as a fraction.

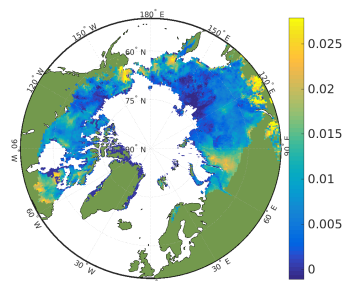
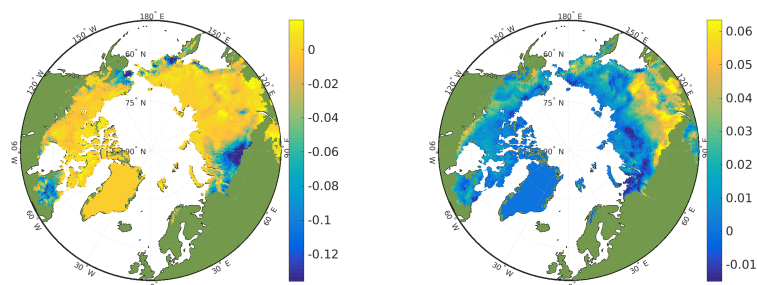
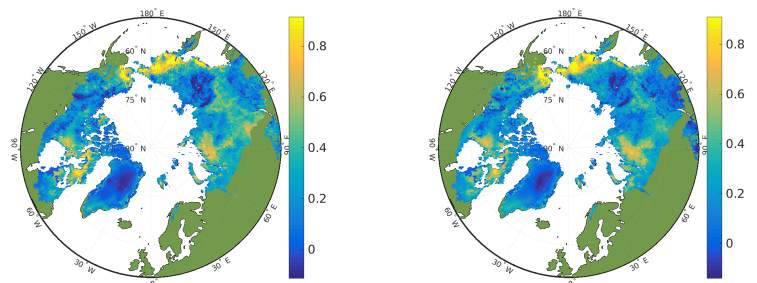


Figure 7: Snow thermal diffusivity relative difference (REDVAR versus CNTL). Numbers are expressed as a fraction.

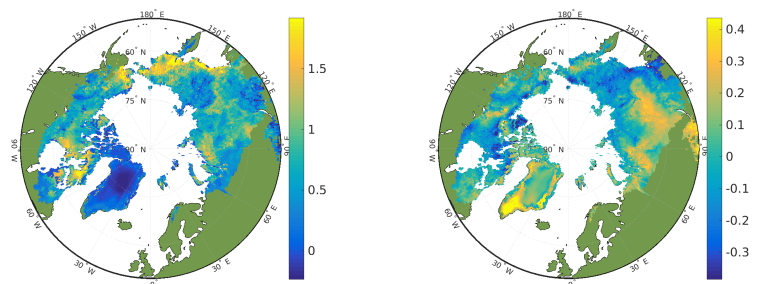


(a) Winter (DJF) lichen and bryophyte thermal diffusivity relative difference. (b) Summer (JJA) lichen and bryophyte thermal diffusivity relative difference.

Figure 8: Comparison of lichen and bryophyte 1980-2009 average properties (REDVAR versus CNTL). Numbers are expressed as a fraction.

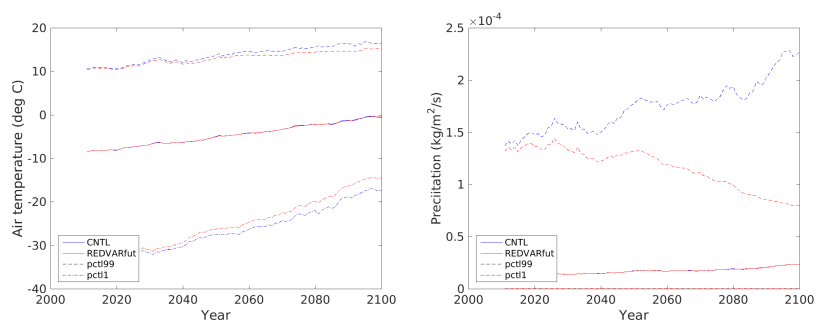


(a) Annual topsoil temperature difference (°C). (b) Annual subsoil temperature difference (°C).

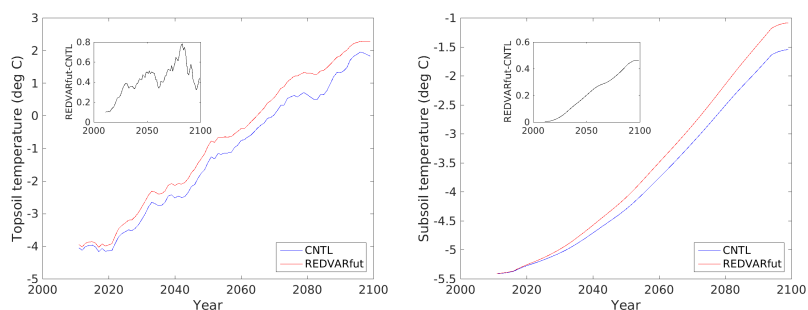


(c) Winter (DJF) topsoil temperature difference (°C). (d) Summer (JJA) topsoil temperature difference (°C).

Figure 9: Comparison of 1980-2009 average soil temperature (REDVAR versus CNTL). Topsoil and subsoil refer to depths of 3 cm and 38 m, respectively.



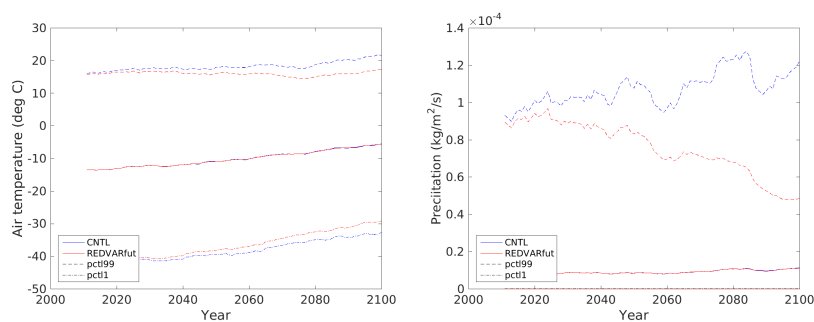
(a) Air temperature (deg C) annual mean, per- (b) Precipitation (kg/m<sup>2</sup>/s) annual mean, per-  
 centile 1 and percentile 99. centile 1 and percentile 99.



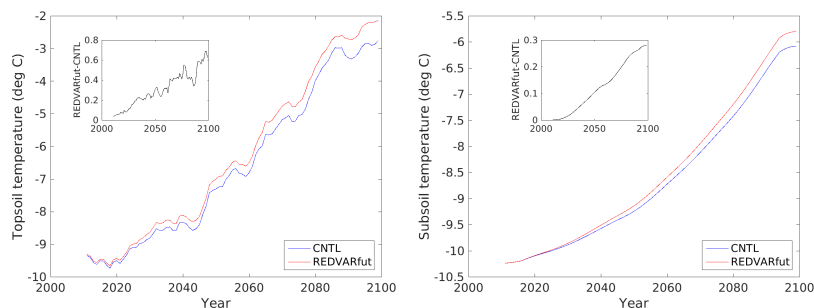
(c) Annual topsoil (3 cm) temperature time series (d) Annual subsoil (38 m) temperature time series  
 (deg C). 10-year running means are shown. Insets (deg C). 10-year running means are shown. Insets  
 show the difference time series. show the difference time series.

Figure 10: REDVARfut experiment results at a Canadian site (62.2N/-75.6E) during 2011-2100 showing the effects of changing climate variability on future soil temperature.





(a) Air temperature (deg C) annual mean, per- (b) Precipitation (kg/m<sup>2</sup>/s) annual mean, per-  
 centile 1 and percentile 99. centile 1 and percentile 99.



(c) Annual topsoil (3 cm) temperature time series (d) Annual subsoil (38 m) temperature time series  
 (deg C). 10-year running means are shown. Insets (deg C). 10-year running means are shown. Insets  
 show the difference time series. show the difference time series.

Figure 11: REDVARfut experiment results at a Siberian site (72.2N/147E) during 2011-2100 showing the effects of changing climate variability on future soil temperature.